Alexandria Engineering Journal (2021) 60, 4213–4222

HOSTED BY

Alexandria University

Alexandria Engineering Journal

www.elsevier.com/locate/aej
www.sciencedirect.com

Marine Predator Algorithm based Cascaded PIDA Load Frequency Controller for Electric Power Systems with Wave Energy Conversion Systems

Ahmed H. Yakout [a], Mahmoud A. Attia [a], Hossam Kotb [b,*]

[a] *Department of Electrical Power and Machines, Faculty of Engineering, Ain Shams University, Cairo, Egypt*
[b] *Department of Electrical Power and Machines, Faculty of Engineering, Alexandria University, Alex., Egypt*

Received 19 November 2020; revised 3 February 2021; accepted 9 March 2021
Available online 21 March 2021

KEYWORDS

Load frequency control;
Cascaded PIDA;
MPA;
Wave energy conversion system;
Two-area interconnected system

Abstract This paper proposes a Cascaded PIDA (Proportional-Integral-Derivative-Acceleration) load frequency controller (LFC) for interconnected power systems with Wave Energy Conversion Systems (WECS). The proposed controller parameters are optimized using the Marine Predator Algorithm (MPA), which is a recent optimization technique known to be robust. The Cascaded PIDA controller results are compared to the results of a single structure MPA based PIDA controller and other PIDA controllers whose parameters are optimized using various optimization techniques presented in previous literature. Results show that the MPA-based PIDA-LFC has better results than other PIDA controllers optimized by other techniques, while the MPA-Cascaded PIDA-LFC has proven to have the best performance where the frequency and the tie-line power fluctuations, due to the connected Wave Energy Conversion System, are efficiently damped. Moreover, the results are presented in the form of time-domain simulation conducted via MATLAB / SIMULINK.

1. Introduction

Maintaining the frequency and tie-line power at constant values upon load and/or generation variations has been one of the major problems of interconnected multi-area power systems. When a load disturbance occurs in one area, it causes frequency deviations not only in the same area but in other connected areas, which makes it necessary to design an effective system controller capable of maintaining the system frequency and the tie-line power flow within the desired limits [1–3]. Such a controller exists and is known as the load frequency controller [4,5]. Load frequency controllers are fed by the area error which is the sum of both the frequency and tie-line power deviations producing correcting signals that change the governor settings of the area generators producing more or less generation in a manner that would stabilize both the frequency of the system and the tie-line power values [6,7].

* Corresponding author.
E-mail addresses: Ahmed.yakout@eng.asu.edu.eg (A.H. Yakout), Mahmoud.abdullah@eng.asu.edu.eg (M.A. Attia), Hossam.kotb@alexu.edu.eg (H. Kotb).

Peer review under responsibility of Faculty of Engineering, Alexandria University.

https://doi.org/10.1016/j.aej.2021.03.011
1110-0168

Various controller structures have been implemented in the literature to improve the performance of the LFC. For example, in [8,9], a Fuzzy logic controller was designed to keep the frequency deviations within acceptable limits for a two-area system with thermal power plants. Whereas a Model Predictive load frequency controller was implemented in [10] to improve the system performance under the uncertainties of turbine and governor parameter variations. While, in [11] a decentralized H-infinity based LFC was proposed to control the frequency of a deregulated power system.

Although, the aforementioned techniques have proven a good system response, the classical PI, PID and other similar controllers were most widely used in LFC design due to their simplicity [12]. For example, in [13], a Particle Swarm Optimization based PI-LFC was presented to improve the response of the studied system when subjected to different step load variations (from 1% to 3%). Moreover, different optimization techniques were proposed to adjust the PID based LFC parameters such as the Genetic Algorithm in [14], Ant colony optimization in [15], Particle Swarm optimization in [16], and Harmony Search algorithm in [17]. Also, a Sine Cosine optimization algorithm based adaptive PID controller was proposed in [18] which provided better performance compared to the conventional PID controller.

Other controllers derived from the PID controller have been used as well. For instance, Fractional Order PID (FOPID) controllers have been implemented by several authors to solve LFC problems in multi-area systems [19–21]. In [22], the FOPID parameters were tuned by fuzzy control for a four-area power system to improve the frequency maximum overshoot and the settling time as well.

Moreover, recently a new type of PID controller known as the PIDA controller where a double derivative (acceleration) branch is added to the conventional PID controller was used in higher-order systems to cope with large overshoots and settling times [23]. Authors in [24] proposed the PIDA structure for load frequency control in a two-area power system and tuned its parameters using the Coefficient Diagram Algorithm improving the overall system frequency stability. Whereas in [25,26], PIDA parameters were tuned using three different optimization algorithms which are the Sine-Cosine Algorithm (SCA), Harmony Search (HS), and Teaching learning-based-optimization (TLBO) methods where, the latest optimized control scheme succeeded in providing better frequency transient response compared to the other techniques.

Furthermore, some researchers have suggested recently the use of cascaded control structures rather than the single structure controller for designing LFC in two-area systems such as the PD-PI structure in [27,28] and the PD-PID structure in [29,30]. The aforementioned cascaded control schemes proved to have better performance by minimizing frequency deviations upon load variation. Moreover, authors in [31] proposed the cascaded PD-FOPID controller which improved the, overshoot, undershoot and settling time of the suggested power system frequency under a load disturbance of 1%. Another cascaded fractional order PI- fractional order PD controller was proposed in [32] which minimized the tie-line power and frequency deviations.

As can be seen, previous literature presented different load frequency controller structures for controlling the frequency of interconnected multi-area power systems. Here, we will combine two recent control structures specifically the Cascaded control structure and the PIDA controller structure to benefit from the advantages of both. Hence, an LFC of a Cascaded PIDA structure is proposed whose parameters (gains) will be optimized using a recent robust optimization technique known as the Marine Predator Algorithm (MPA). The proposed controller will be compared to the MPA-PIDA structure and other structures present in previous literature, specifically the TLBO-PIDA, SCA-PIDA and HS-PIDA controllers [25,26].

The aforementioned controllers will be applied to a two-area power system subjected once to a 1% load variation in area 1 and area 2 simultaneously followed by another study where a fluctuating 15% wave energy conversion system is connected to area 1 while a 1% load disturbance is applied to area 2 simultaneously. Hereby, evaluating the performance of the proposed cascaded PIDA-LFC in the presence of high penetration of renewable energy resources.

Finally, the paper consists of seven sections: Section1 introduces the research topic, while Section 2 presents the case study. Moreover, Section 3 discusses the structure, concept and advantages of the proposed controller. This is followed by the problem formulation and a summary of the proposed optimization technique in Sections 4 and 5. Both results and discussion are presented in Section 6. While, Section 7 concludes the paper.

2. System case study

Our case study is shown in Fig. 1, which consists of two areas interconnected together by a tie-line transferring power from Area-1 to Area-2. Each area is represented by a governor, turbine, generator, and load. All the system components are assumed as linear models using the first-order transfer functions as represented in Fig. 1. Moreover, each area is equipped with a Cascaded PIDA-LFC to control the areas frequency and maintain the system stability when subjected to step disturbances and/or wave energy fluctuations.

3. The proposed controller

In this paper, the cascaded PIDA control scheme is proposed which combines two recent control structures specifically the cascade control structure and the PIDA controller structure to benefit from the advantages of both.

The cascade control is an implementation that can allow the system to be more responsive to disturbances and less susceptible to downtime by using multiple control loops which monitor multiple signals for one manipulated variable [33]. This improves the system performance by achieving rapid damping and/or elimination of the effect of disturbances before it can propagate to other parts of the system. The simple cascade control system includes two control loops (inner and outer) similar to Fig. 2. The outer controller $G_{c1}(s)$ is the primary controller that minimizes the area error in our case, while the inner controller $G_{c2}(s)$ is the secondary controller fed by a biased frequency signal to enhance the system performance under the disturbance effect.

The inner control loop is closer to the disturbance and designed to respond quicker than the outer loop which allows the system to correct its response under different perturbations and system parameters variations.

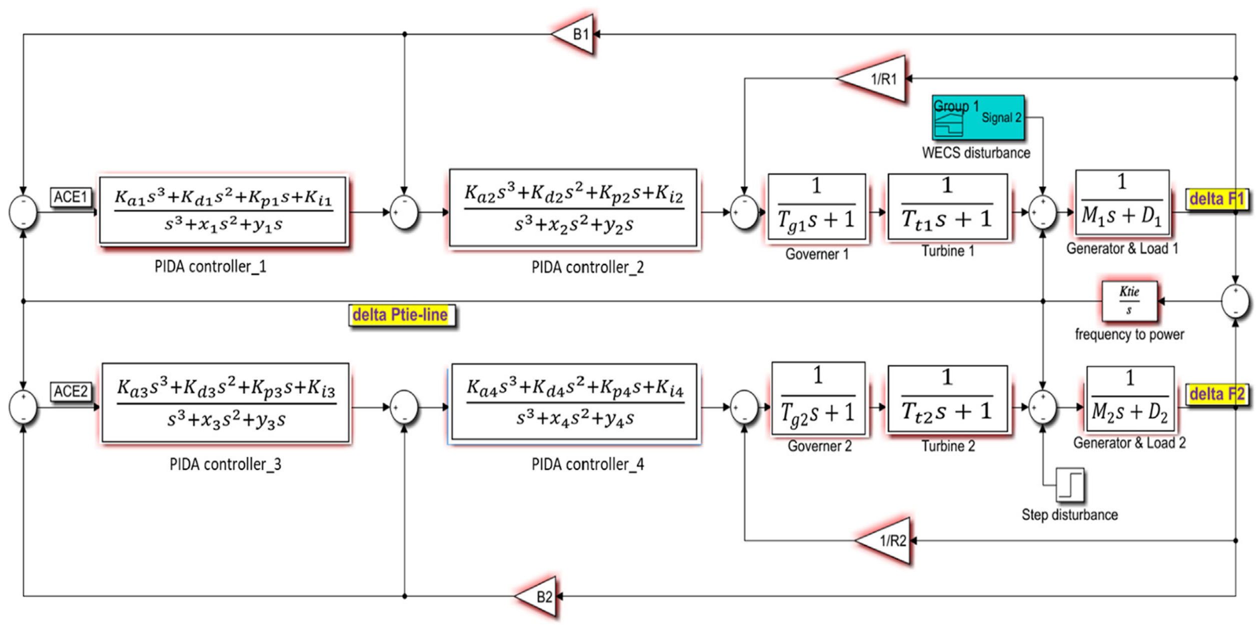

Fig. 1 Block diagram of the two-area case study system equipped with Cascaded PIDA controller.

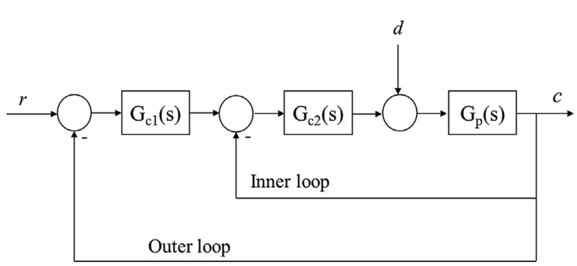

Fig. 2 Block diagram of the cascaded control structure.

In this paper, $G_{c1}(s)$ and $G_{c2}(s)$ are designed as PIDA controllers and each controller has six parameters that must be optimized. The transfer function of the suggested PIDA model is represented in Equation (1), where K_a, K_i, K_d and K_p are the acceleration, integral, derivative, and proportional gains, respectively, while α and β are the filter parameters. The transfer function can be alternatively expressed in the form of a polynomial as given in Equation (2) with the following coefficients K_a, K_i, K_d, K_p, x and y respectively [34].

$$G_c(s) = K_p + \frac{K_i}{s} + \frac{K_d s}{s+\alpha} + \frac{K_a s^2}{(s+\alpha)(s+\beta)} \tag{1}$$

$$G_c(s) = \frac{K_a s^3 + K_d s^2 + K_p s + K_i}{s^3 + x s^2 + y s} \tag{2}$$

The additional acceleration term of the PIDA adds two extra zeros and filters to the system which helps in enhancing the transient response and the settling time. When combined with the cascaded structure, the system stability and transient response would enhance further. Moreover, to show the robust performance of the proposed Cascaded PIDA controller design to wave energy uncertainties, an irregular wave power signal shown in Fig. 3 will be applied to Area-1 while a 1% load disturbance is applied simultaneously to Area-2.

The power fluctuation produced by the WECS (P_w) is expressed in p.u. by Equation (3).

$$P_w = 0.1\mathrm{Sin}\left(\frac{2\pi t}{12}\right) + 0.05\mathrm{Sin}\left(\frac{\pi t}{12}\right) \tag{3}$$

4. Problem formulation

The main objective of the Cascaded PIDA controller design is to minimize the frequency deviation in Area-1 (ΔF_1), the frequency deviation in in Area-2 (ΔF_2), and the tie-line power deviation between the two areas ($\Delta P_{tie-line}$) when certain

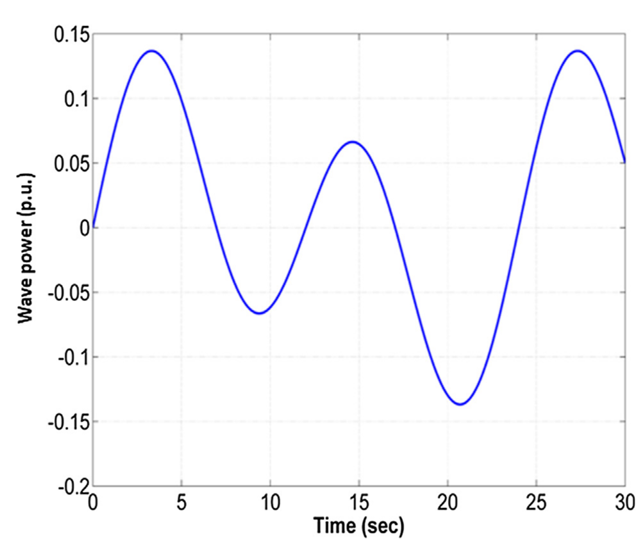

Fig. 3 The proposed WECS power fluctuations.

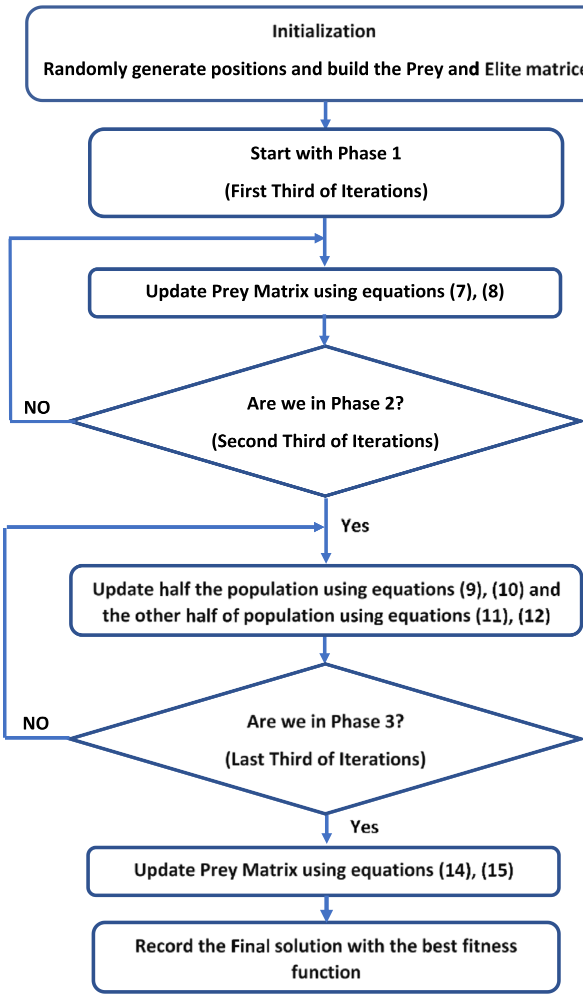

Fig. 4 Flow chart of the MPA optimization method.

disturbances occur in the two areas. Hence, the optimization problem can be summarized as finding the cascaded PIDA-LFC parameters (*Ka,Kd,Kp,Ki,x,y*) that will minimize the following fitness function (*FF*):

$$FF = \int_0^{t_{sim}} (ACE_1{}^2 + ACE_2{}^2)dt \quad (4)$$

where t_{sim}, ACE_1 and ACE_2 are the simulation time in seconds and the Area Control Error of Area-1 and Area-2, respectively.

$$ACE_1 = \Delta P_{tie-line} + B_1 \Delta F_1 \quad (5)$$

$$ACE_2 = \Delta P_{tie-line} + B_2 \Delta F_2 \quad (6)$$

where B_1 and B_2 are the frequency biasing coefficients for Area-1 and Area-2, respectively.

Moreover, the tuning of the PIDA parameters is carried out using the MPA optimization method (discussed in the following section) with the following constraints given in [26,35] suggested for high order power systems and for the sake of a fair comparison with previous work:

$50 \le K_a \le 150$, $200 \le K_i \le 500$, $200 \le K_d \le 1000$
$500 \le K_p \le 1000$, $300 \le x \le 800$, $500 \le y \le 1500$

5. Marine predator Algorithm (MPA)

MPA is an optimization technique inspired by the movement of marine predators when searching for prey. Two popular identified predator types of movements are, the Levy movement and the Brownian movement. The Levy motion consists of short steps followed by high jumps that enhance exploration. Whereas the Brownian motion consists of fixed steps in the same vacancy to optimize exploitation. Fig. 4 shows the main steps of MPA technique which can be summarized as follows; For more details, check [36]:

1. Initialization: Two matrices are constructed, the *Prey matrix* which consists of the proposed variable random positions during the initialization process and the *Elite matrix* which consists of the position vector with best fitness function repeated.

2. Phase (1), the first third of iterations: The prey moves using the Brownian movement, updating the Prey matrices as follows:

$$\overrightarrow{step_i} = \overrightarrow{R_B} \otimes (\overrightarrow{Elite_i} - (\overrightarrow{R_B} \otimes \overrightarrow{Prey_i})) \quad (7)$$

$$\overrightarrow{Prey_i} = \overrightarrow{Prey_i} + (P.\overrightarrow{R} \otimes \overrightarrow{Step_i}) \quad (8)$$

Where $P = 0.5$, R is a vector of uniform random number between [0, 1] and R_B is a vector containing random numbers based on normal distribution of Brownian motion.

3. Phase (2), the second third of iterations: The predator moves using Brownian while the prey moves using Levy movement and the first half of the population is updated as follows:

$$\overrightarrow{step_i} = \overrightarrow{R_L} \otimes (\overrightarrow{Elite_i} - (\overrightarrow{R_L} \otimes \overrightarrow{Prey_i})) \quad (9)$$

$$\overrightarrow{Prey_i} = \overrightarrow{Prey_i} + (P.\overrightarrow{R} \otimes \overrightarrow{Step_i}) \quad (10)$$

Table 1 Optimized gains of the PIDA controller based on different optimization techniques for 1% step load disturbances in Area-1 and Area-2.

	HS [25]		SCA [25]		TLBO [25]		MPA (proposed)	
PIDA	Area-1	Area-2	Area-1	Area-2	Area-1	Area-2	Area-1	Area-2
K_a	130.5	138.5	139.3	139.7	143.8	138.2	150	150
K_d	534.8	520.4	499.5	513.3	540.3	510.5	999.9	1000
K_p	801.7	818.7	850	796.9	774.4	788.6	999.9	899.9
K_i	429.4	369.2	384.3	445.2	415.2	408.3	499.9	499.9
x	597	626	574.2	603.4	551.7	573	300	300
y	934	957.5	994	997.2	981.1	932.1	500	500.01
FF	2.8738e-4		2.8938e-4		2.7810e-4		8.8257e-5	

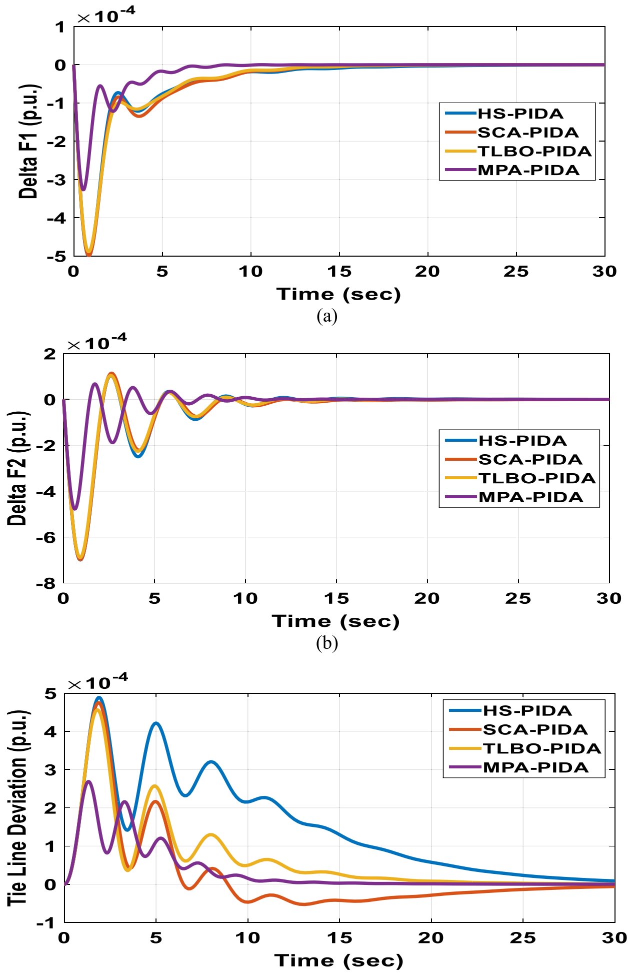

(c)

Fig. 5 (a) Frequency deviation in Area-1, (b) Frequency deviation in Area-2 and (c) Tie-line power deviation for 1% simultaneous step load disturbances in both areas using PIDA controller based on different optimization algorithms.

Where R_L is a vector containing random numbers based on levy's motion normal distribution. While the other half of population is updated as follows:

$$\overrightarrow{step_i} = \overrightarrow{R_B} \otimes ((\overrightarrow{R_B} \otimes \overrightarrow{Elite_i}) - \overrightarrow{Prey_i}) \tag{11}$$

$$\overrightarrow{Prey_i} = \overrightarrow{Elite_i} + (P.CF \otimes \overrightarrow{Step_i}) \tag{12}$$

Where the Elite matrix is multiplied by R_B and CF is as follows:

$$CF = [1 - (Iter./Max.Iter.)]^{(2.Iter./Max.Iter.)} \tag{13}$$

4. Phase (3), the last third of iterations: The predator moves using Levy motion, and the Prey matrix is updated as follows:

$$\overrightarrow{\mathrm{step_i}} = \overrightarrow{\mathrm{R_L}} \otimes ((\overrightarrow{\mathrm{R_L}} \otimes \overrightarrow{\mathrm{Elite_i}}) - \overrightarrow{\mathrm{Prey_i}}) \tag{14}$$

$$\overrightarrow{Prey_i} = \overrightarrow{Elite_i} + (P.CF \otimes \overrightarrow{Step_i}) \tag{15}$$

5. Finalizing: After each iteration, the Elite matrix is updated with the best solutions and the final solution will be presented after the last iteration.

6. Results and discussion

The simulation results are organized into 5 main sections as follows, where the MPA-PIDA controller is compared to other optimization techniques followed by comparing our proposed MPA based cascaded-PIDA controller with the single MPA-PIDA discussed earlier. Then robustness of our proposed controller will be discussed under different load step perturbations, changes in system parameters and with an irregular wave energy conversion system.

6.1. MPA-PIDA model compared to previous applied techniques

This section presents the results of the proposed MPA-PIDA model to previous optimization techniques presented in [25] such as the HS-PIDA, SCA-PIDA and TLBO-PIDA models for 1% step load disturbances occurring simultaneously in both Areas 1 and 2. Table 1 shows the optimized gains of the PIDA controller based on different optimization techniques [25]. It can be observed that the proposed MPA method gives the best (least) fitness function (FF) compared to other techniques. By applying these gains to the case study model,

Table 3 Optimized gains of the MPA-Cascaded PIDA controller for 1% step load disturbances in Area-1 and Area-2.

Cascaded-PIDA	Area-1		Area-2	
	Outer loop	Inner loop	Outer loop	Inner loop
K_a	149.99	149.4	149.7	149.93
K_d	996.4	999.64	999.27	999.72
K_p	999.63	1000	1000	1000
K_i	496.27	499.54	499.57	499.97
x	306.07	313.68	300.02	300.22
y	579.14	515.06	850.88	500
FF	1.2133e-5			

Table 2 Transient response specifications of different optimization techniques based PIDA controller for 1% step load disturbance in Area-1 and 2.

Optimization Techniques	HS [25]			SCA [25]			TLBO [25]			MPA (proposed)		
Variables	ΔF_1	ΔF_2	ΔP_{tie}	ΔF_1	ΔF_2	ΔP_{tie}	ΔF_1	ΔF_2	ΔP_{tie}	ΔF_1	ΔF_2	ΔP_{tie}
Overshoot (p.u.) X10^{-4}	——	1.04	4.88	——	1.14	4.75	——	1.04	4.56	——	0.67	2.68
Undershoot (p.u.) X10^{-4}	−4.9	−6.9	——	−4.9	−6.9	−0.52	−4.89	−6.8	——	−3.2	−4.7	——
Settling Time (sec)	15	15	30	15	15	30	15	15	30	10	12	15

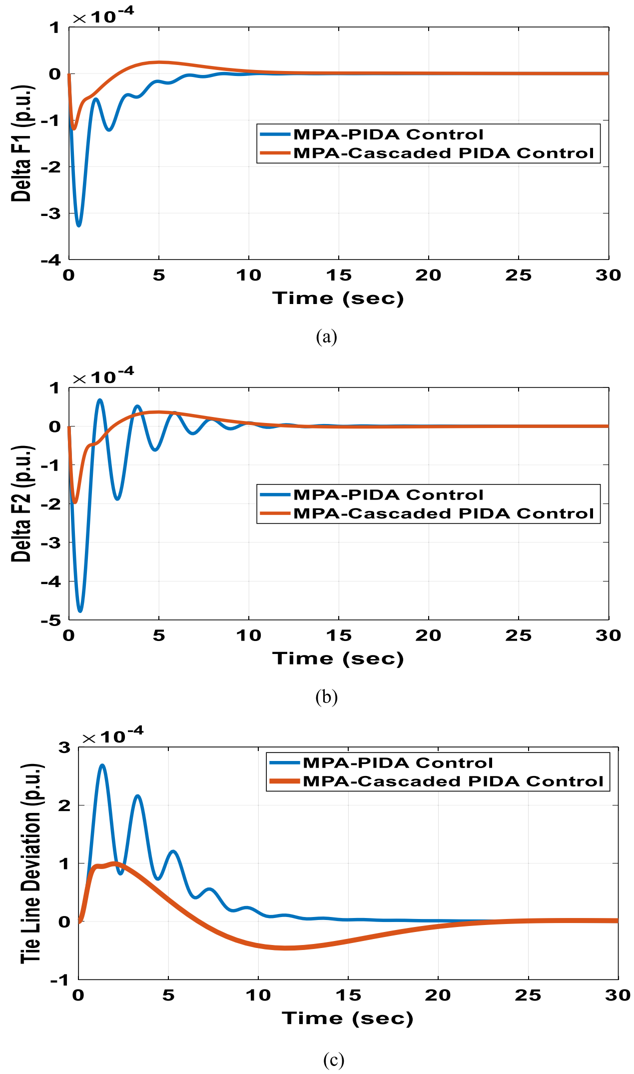

Fig. 6 (a) Frequency deviation in Area-1, (b) Frequency deviation in Area-2 and (c) Tie-line power deviation for 1% simultaneous step load disturbances in both areas using MPA based PIDA and Cascaded PIDA.

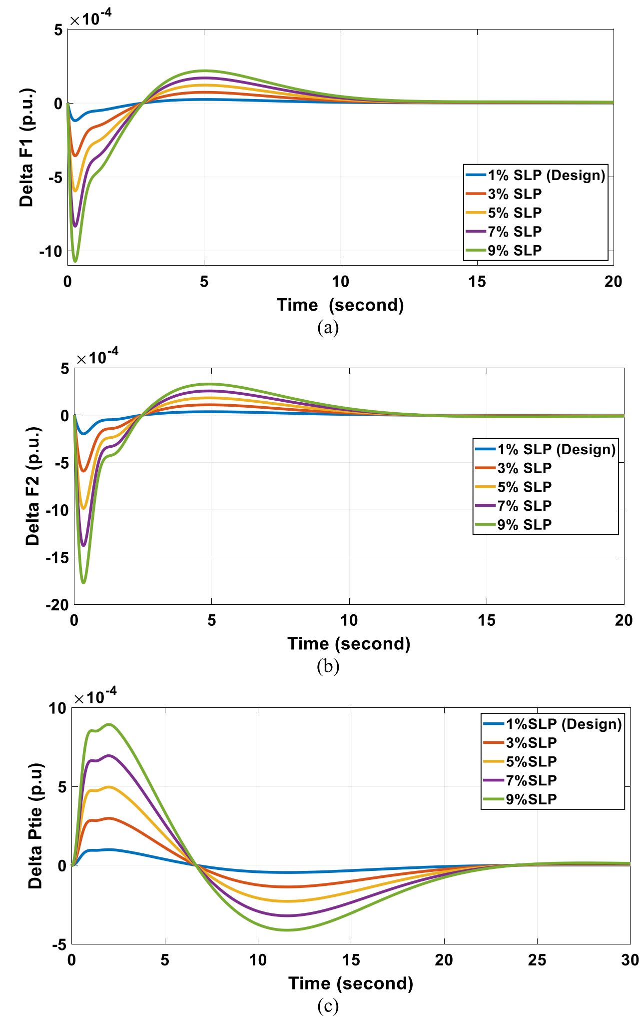

Fig. 7 (a) Frequency deviation in Area-1, (b) Frequency deviation in Area-2 and (c) Tie-line power deviation for different SLP.

the system response can be improved as shown in Fig. 5 under 1% step load disturbance in Area-1 and Area-2 simultaneously.

As shown in Fig. 5, the PIDA based on MPA method has a better transient response compared to other techniques. Also, the performance of the MPA-PIDA model has the lowest settling time of about 10, 12 and 15 sec for ΔF_1, ΔF_2 and $\Delta P_{tie-line}$, respectively. Moreover, Fig. 5 (a) and (b), show that the MPA-PIDA response has a lower undershoot than the other techniques which is -3.2×10^{-4}p.u for ΔF_1 and -4.7×10^{-4}p.u for ΔF_2. Also, the MPA-PIDA case has a lower overshoot than the other cases when considering the tie-line power deviation ($\Delta P_{tie-line}$) which equals 2.68×10^{-4}p.u (see Fig. 5 (c)). Other techniques based PIDA have approximately the same ΔF_1 and ΔF_2 responses but with different $\Delta P_{tie-line}$ response. The transient response specifications (settling time, overshoot, undershoot) of the PIDA design based on different optimization techniques are summarized in Table 2.

Table 4 Transient response specifications of MPA based PIDA and Cascaded PIDA controllers for 1% step load disturbance in Area-1 and 2.

Controller Structure	MPA-PIDA			MPA-Cascaded PIDA		
Variables	ΔF_1	ΔF_2	ΔP_{tie}	ΔF_1	ΔF_2	ΔP_{tie}
Overshoot (p.u.)$\times 10^{-4}$	——	0.67	2.68	0.24	0.36	0.993
Undershoot (p.u.)$\times 10^{-4}$	− 3.2	− 4.7	——	− 1.19	− 1.9	− 0.45
Settling time (sec)	10	12	15	10	12	21

6.2. MPA-PIDA model compared to the proposed MPA-Cascaded PIDA

Since the MPA method has proved its superiority over other techniques, this section will compare the results of using MPA with both PIDA and the proposed cascaded PIDA LFCs. Table 3 shows the optimum values of the Cascaded PIDA gains for inner and outer loops controllers based on the MPA optimization method. It can be observed that the fitness function (FF) of the cascaded PIDA is much lower than that of the PIDA obtained in Table 1 which means that the system response is greatly improved by using the cascaded PIDA as shown in Fig. 6.

By applying 1% step load disturbance in both areas 1 and 2 simultaneously, the Cascaded PIDA model has a better transient response than single PIDA controller in terms of the max. overshoot and min. undershoot. Both controllers have approximately the same settling of about 10 and 12 sec for ΔF_1 and ΔF_2, respectively. For $\Delta P_{tie\text{-}line}$, the settling time of the MPA-PIDA is 15 sec which is slightly lower than the settling time of the MPA-Cascaded PIDA which equals 21 sec. For example, in Fig. 6 (a), the MPA-Cascaded PIDA has a lower undershoot and overshoot which are -1.2×10^{-4}p.u and 0.24×10^{-4}p.u for ΔF_1. However, the PIDA controller exhibits only higher undershoot in ΔF_1 that accounts for -3.2×10^{-4}p.u. Moreover, the system response with MPA based cascade PIDA exhibits less oscillations. The transient response specifications of the MPA-PIDA and MPA-Cascaded PIDA controllers for 1% step load disturbance in Area-1 and 2 are summarized in Table 4.

6.3. Evaluation of the system performance under different step load perturbations (SLP) using the proposed MPA-cascaded PIDA controller

This case study aims to evaluate the robustness stability and performance of the proposed controller under various step load disturbances. By applying different SLP ratios of 1, 3, 5, 7, and 9% to the double area system, the dynamic responses of ΔF_1, ΔF_2 and $\Delta P_{tie\text{-}line}$ can be obtained as illustrated in Fig. 7(a)-(c). The system exhibits some allowable overshoot

Table 5 Transient response specifications of MPA-Cascaded PIDA controller for different SLP.

SLP %	ΔF_1		ΔF_2		ΔP_{tie}	
	Undershoot (pu)$\times10^{-4}$	Overshoot (pu)$\times10^{-4}$	Undershoot (pu)$\times10^{-4}$	Overshoot (pu)$\times10^{-4}$	Undershoot (pu)$\times10^{-4}$	Overshoot (pu)$\times10^{-4}$
1(Design value)	−1.19	0.243	−1.9	0.366	−0.458	0.993
3	−4	0.728	−6	1.098	−1.373	2.978
5	−6	1.214	−10	1.83	−2.289	4.963
7	−8	1.700	−14	2.562	−3.205	6.948
9	−11	2.185	−18	3.294	−4.12	8.933

Table 6 Dynamic response specifications of MPA-Cascaded PIDA controller for system parameters change.

System parameter	Percentage of change	ΔF_1		ΔF_2		ΔP_{tie}	
		US (pu)$\times10^{-4}$	OS (pu)$\times10^{-4}$	US (pu)$\times10^{-4}$	OS (pu)$\times10^{-4}$	US (pu)$\times10^{-4}$	OS (pu)$\times10^{-4}$
T_{t1}	−25%	−0.998	0.24	−1.969	0.3633	−0.4451	1.093
	25%	−1.364	0.2466	−1.972	0.3685	−0.4712	0.935
T_{t2}	−25%	−1.189	0.2389	−1.672	0.36	−0.4753	0.905
	25%	−1.191	0.2467	−2.237	0.3761	−0.4499	1.297
T_{g1}	−25%	−1.05	0.2434	−1.969	0.3649	−0.4519	1.011
	25%	−1.1322	0.2424	−1.972	0.367	−0.4638	0.977
T_{g2}	−25%	−1.189	0.2408	−1.725	0.3656	−0.4654	0.961
	25%	−1.191	0.2448	−2.193	0.3667	−0.451	1.169
$1/R_1$	−25%	−1.195	0.2577	−1.971	0.3677	−0.4813	0.942
	25%	−1.186	0.23	−1.97	0.3645	−0.4386	1.041
$1/R_2$	−25%	−1.19	0.2453	−1.978	0.3908	−0.426	1.079
	25%	−1.19	0.2406	−1.963	0.3453	−0.4901	0.912
B_1	−25%	−1.469	0.3229	−1.973	0.3524	−0.1799	0.517
	25%	−1.006	0.1943	−1.969	0.3752	−0.6306	1.371
B_2	−25%	−1.91	0.229	−2.386	0.4797	−0.9551	1.774
	25%	−1.189	0.2528	−1.689	0.2957	−0.1946	0.49
M_1	−25%	−1.268	0.2374	−1.974	0.3661	−0.459	1.009
	25%	−1.132	0.2484	−1.968	0.3658	−0.4569	0.978
M_2	−25%	−1.194	0.2429	−2.13	0.3579	−0.4552	0.967
	25%	−1.187	0.2427	−1.852	0.3745	−0.4608	1.017

and undershoot oscillations and these oscillations increase by increasing the SLP ratio. However, these oscillations are still within the acceptable range of the frequency and tie-line power deviations. Also, it can be found that the settling time is not affected by changing the load perturbation. The transient response specifications for this case are given in Table 5 in terms of undershoot and overshoot values. This confirms the ability of the MPA-Cascaded PIDA controller to maintain a stable system response with fewer oscillations for different load disturbances.

6.4. Sensitivity analysis to system parameters change:

Moreover, additional analysis is implemented to evaluate the sensitivity of the proposed controller to system parameters change. The transient response characteristics are shown in Table 6 by changing all the system parameters by ± 25%. This analysis considers the effect of varying the turbines time constants (T_{t1}, T_{t2}), the governor time constants (T_{g1}, T_{g2}), the speed droops (R_1, R_2), the frequency bias coefficients (B_1, B_2) and the generator constants (M_1, M_2). When the system parameters change, the undershoot (US) and overshoot (OS) oscillations is found to vary slightly within an acceptable range for ΔF_1, ΔF_2 and $\Delta P_{tie\text{-}line}$. In addition, the settling time of the system response doesn't change significantly and hence not included in Table. This confirms the robustness of our proposed scheme.

6.5. Performance of controllers under irregular WECS fluctuations

This section compares the results of MPA-PIDA and MPA-Cascaded PIDA LFCs with the previously presented TLBO-PIDA LFC [26] (best of previous literature) when applying a fluctuating 15% wave energy conversion system to Area-1 and 1% step disturbance in Area-2, simultaneously. As illustrated in Table 7, the best fitness function (FF) under the effect of WECS can be obtained by using the suggested MPA-Cascaded PIDA model.

As shown in Fig. 8, the MPA-Cascaded PIDA controller has a better transient response compared to the MPA-PIDA and TLBO-PIDA controllers under the effect of WECS disturbance. Furthermore, the Cascaded PIDA controller sufficiently damps the effect of the wave system fluctuations resulting in fewer ripples for ΔF_1, ΔF_2 and $\Delta P_{tie\text{-}line}$ when compared to the other PIDA controllers. It can be seen that the frequency and tie-line power deviations approach zero by using the Cascaded PIDA controller indicating that the system is nearly not affected by the wave energy fluctuations.

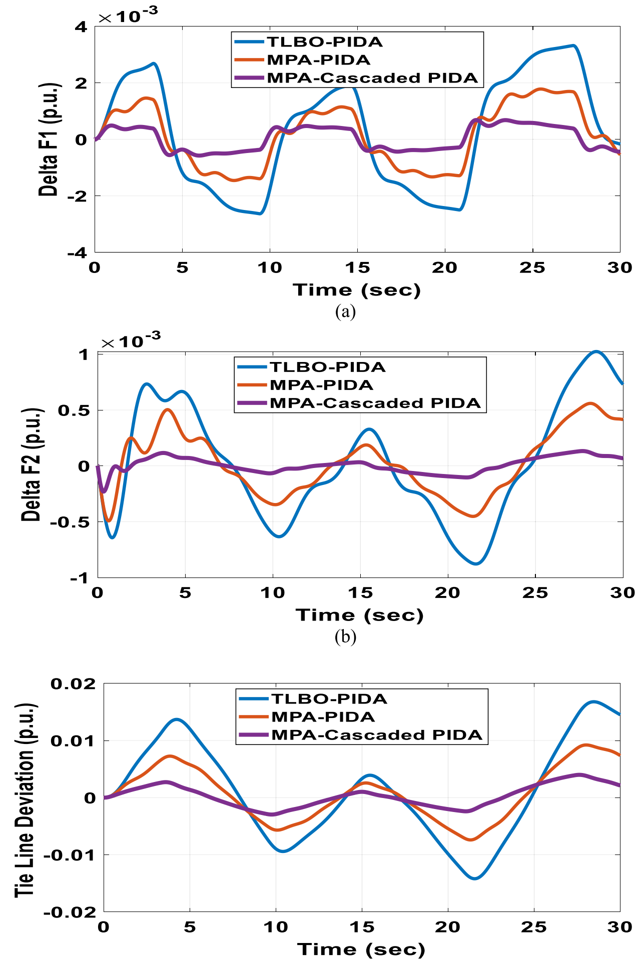

Fig. 8 (a) Frequency deviation in Area-1, (b) Frequency deviation in Area-2 and (c) Tie-line power deviation under WECS in Area-1 and 1% step disturbance in Area-2 for different control models.

Table 7 Optimized gains of different control models under the effect of WECS in Area-1 and 1% step disturbance in Area-2.

	TLBO-PIDA [26]		MPA-PIDA		MPA-Cascaded PIDA			
	Area-1	Area 2	Area 1	Area 2	Area 1		Area 2	
					Outer loop	Inner loop	Outer loop	Inner loop
K_a	143.8	138.2	150	150	149.99	149.4	149.7	149.93
K_d	540.3	510.5	999.9	1000	996.4	999.64	999.27	999.72
K_p	774.4	788.6	999.9	899.9	999.63	1000	1000	1000
K_i	415.2	408.3	499.9	499.9	496.27	499.54	499.57	499.97
x	551.7	573	300	300	306.07	313.68	300.02	300.22
y	981.1	932.1	500	500.01	579.14	515.06	850.88	500
FF	0.0594		0.00008		0.000012			

7. Conclusion

In this paper, the load frequency control of a two-area interconnected system is improved using MPA based Cascaded PIDA-LFC. First, the MPA based single PIDA controller has proven its superiority over other PIDA structures optimized using previous optimization techniques specifically HS, SC and TLBO. Next, the MPA based Cascaded PIDA controller is proposed and shows a better transient response than single structure PIDA controller in terms of overshoot and undershoot percentages. Moreover, the robustness of the MPA-Cascaded PIDA controller is verified at different step load perturbations and $\pm 25\%$ system parameters variations. Finally, the system response has been improved using the Cascaded PIDA controller when subjecting to an irregular fluctuating WECS where the system frequency and tie-line power deviations are successfully minimized compared to other structures.

Declaration of Competing Interest

The authors declare that they have no known competing financial interests or personal relationships that could have appeared to influence the work reported in this paper.

References

[1] B. Mohanty, S. Panda, P.K. Hota, Controller parameters tuning of differential evolution algorithm and its application to load frequency control of multi-source power system, Int. j. electr. power energy syst. 54 (2014) 77–85.

[2] A. Pappachen, A. Peer Fathima, Critical research areas on load frequency control issues in a deregulated power system: A state-of-the-art-of-review, Renew. Sustain. Energy Rev. 72 (2017) 163–177.

[3] S.D. Hanwate, Y.V. Hote, Optimal PID design for Load frequency control using QRAWCP approach, IFAC-PapersOnLine. 51 (4) (2018) 651–656.

[4] E. Rakhshani, J. Sadeh, Practical viewpoints on load frequency control problem in a deregulated power system, Energy Convers. Manag. 51 (6) (2010) 1148–1156.

[5] S. Jain, Y.V. Hote, Generalized active disturbance rejection controller for load frequency control in power systems, IEEE Control Syst. Lett. 4 (1) (2020) 73–78.

[6] H.A. Yousef, Power system load frequency control: Classical and adaptive fuzzy approaches, Productivity Press, New York, NY, 2017.

[7] H. Alhelou, M.-E. Hamedani-Golshan, R. Zamani, E. Heydarian-Forushani, P. Siano, Challenges and opportunities of Load Frequency Control in conventional, modern and future smart power systems: A comprehensive review, Energies. 11 (10) (2018) 2497–2532.

[8] S.R. Khuntia, S. Panda, Simulation study for automatic generation control of a multi-area power system by ANFIS approach, Appl. Soft Comput. 12 (1) (2012) 333–341.

[9] A. Dokht Shakibjoo, M. Moradzadeh, S.Z. Moussavi, H. Afrakhte, Online adaptive type-2 fuzzy logic control for load frequency of multi-area power system, J. Intell. Fuzzy Syst. 37 (1) (2019) 1033–1042.

[10] X. Liu, Y. Zhang, K.Y. Lee, "Robust distributed MPC for load frequency control of uncertain power systems, Control Eng. Pract. 56 (2016) 136–147.

[11] R.A. Davidson, S. Ushakumari, H-infinity loop-shaping controller for load frequency control of a deregulated power system, Procedia technol. 25 (2016) 775–784.

[12] Y.V. Hote, S. Jain, PID controller design for load frequency control: Past, Present and future challenges, IFAC-PapersOnLine. 51 (4) (2018) 604–609.

[13] K.P. SinghParmar, PSO based PI controller for the LFC system of an interconnected power system, Int. J. Comput. Appl. 88 (7) (2014) 20–25.

[14] A. Saxena, M. Gupta, V. Gupta, Automatic generation control of two area interconnected power system using Genetic algorithm, in 12th IEEE International Conference on Computational Intelligence and Computing Research, 2012.

[15] M. Omar, M. Solimn, A. Abdelghany, F. Bendary, Optimal tuning of PID controllers for hydrothermal load frequency control using ant colony optimization, Int. J. Electr. Eng. Inform. 5 (3) (2013) 348–360.

[16] N.K. Bahgaat, M.I. El-Sayed, M.A.M. Hassan, F.A. Bendary, Load Frequency Control in power system via improving PID controller based on Particle Swarm Optimization and ANFIS techniques, Int. J. Syst. Dyn. Appl. 3 (3) (2014) 1–24.

[17] M. Omar, M.A. Ebrahim, A. Abdelghany, F. Bendary, Tuning of PID Controller for Load Frequency Control Problem via Harmony Search Algorithm, Ind. J. Elec. Eng. Com. Sc. 1 (2) (2016) 255–263.

[18] K.S. Rajesh, S.S. Dash, Load frequency control of autonomous power system using adaptive fuzzy based PID controller optimized on improved sine cosine algorithm, J. Ambient Intell. Humaniz. Comput. 10 (6) (2019) 2361–2373.

[19] S. Sondhi, Y.V. Hote, Fractional order PID controller for perturbed load frequency control using Kharitonov's theorem, Int. j. electr. power energy syst. 78 (2016) 884–896.

[20] A. Delassi, S. Arif, L. Mokrani, Load frequency control problem in interconnected power systems using robust fractional PIλD controller, Ain Shams Eng. J. 9 (1) (2018) 77–88.

[21] R. Lamba, S.K. Singla, S. Sondhi, Design of fractional order PID controller for load frequency control in perturbed two area interconnected system, Electr. Power Compon. Syst. 47 (11) (2019) 998–1011.

[22] M.M. Ismail, A.F. Bendary, Load frequency control for multi area smart grid based on advanced control techniques, Alex. Eng. J. 57 (4) (2018) 4021–4032.

[23] M. Kumar, Y.V. Hote, Robust IMC-PIDA controller design for load frequency control of a time delayed power system, in 58th IEEE Conference on Decision and Control (CDC), 2019.

[24] M. Kumar, Y.V. Hote, "Robust CDA-PIDA control scheme for load frequency control of interconnected power systems, IFAC-PapersOnLine. 51 (4) (2018) 616–621.

[25] M.M. Elsaied, M.A. Mostafa, S.F. Mekhamer, M.A. Attia, Application of different optimization techniques to load frequency control in a multi-area system, in 19th International Middle East Power Systems Conference (MEPCON), 2017.

[26] M. Mostafa Elsaied, M. Abdallah Attia, M. Abdelhamed Mostafa, S. Fouad Mekhamer, Application of different optimization techniques to load frequency control with WECS in a multi-area system, Electr. Power Compon. Syst. 46 (7) (2018) 739–756.

[27] S. Panda, N.P. Patidar, M. Kolhe, Cascaded PD-PI controller for active power frequency control of two-area multi-units power system, in 16th IEEE International Conference on Power and Renewable Energy (ICPRE), 2016.

[28] D. Tripathy, N.B.D. Choudhury, B.K. Sahu, A novel cascaded fuzzy PD-PI controller for load frequency study of solar-thermal/wind generator-based interconnected power system using grasshopper optimization algorithm, Int. J. Electr. Eng. Educ. (2020) 1–18.

[29] P. Dash, L.C. Saikia, N. Sinha, Automatic generation control of multi area thermal system using Bat algorithm optimized PD–PID cascade controller, Int. J. Electr. Power Energy Syst. 68 (2015) 364–372.

[30] P. Satapathy, M. K. Debnath, N. Charan Patel, P. K. Mohanty, Load frequency control with PDPID controller including double derivative filter, in International Conference on Recent Innovations in Electrical, Electronics & Communication Engineering (ICRIEECE), 2018.

[31] B. Shaw, J.R. Nayak, Ant Lion Optimizer Optimized Cascade PD-FPID Controller Based AGC in Deregulated Environment, Int. J. Ind. Control Sys. Security. 2 (1) (2017) 64–72.

[32] E. Çelik, Design of new fractional order PI–fractional order PD cascade controller through dragonfly search algorithm for advanced load frequency control of power systems, Soft Comput (2020).

[33] G.L. Raja, A. Ali, Series cascade control: An outline survey, Indian Control Conference (ICC). IEEE (2017).

[34] D. Sambariya, D. Paliwal, Comparative design and analysis of PIDA controller using kitti's and Jung-dorf approach for third order practical systems, Br. J. Math. Comput. Sci. 16 (5) (2016) 1–16.

[35] D. Puangdownreong, Application of current search to optimum PIDA controller design, Intelligent Control and Automation 03 (04) (2012) 303–312.

[36] A. Faramarzi, M. Heidarinejad, S. Mirjalili, A.H. Gandomi, Marine Predators Algorithm: A nature-inspired metaheuristic, Expert Syst. Appl. 152 (2020) 1–28.